NASA Technical Memorandum 101340

Dynamic Porosity Variations in Ceramics

Edward R. Generazio
National Aeronautics and Space Administration
Lewis Research Center
Cleveland, Ohio

David B. Stang
Sverdrup Technology, Inc.
NASA Lewis Research Center Group
Cleveland, Ohio

and

Don J. Roth
National Aeronautics and Space Administration
Lewis Research Center
Cleveland, Ohio

December 1988

NASA

DYNAMIC POROSITY VARIATIONS IN CERAMICS

Edward R. Generazio
National Aeronautics and Space Administration
Lewis Research Center
Cleveland, Ohio 44135

David B. Stang
Sverdrup Technology, Inc.
NASA Lewis Research Center Group
Cleveland, Ohio 44135

Don J. Roth
National Aeronautics and Space Administration
Lewis Research Center
Cleveland, Ohio 44135

Summary

A silicon carbide disk was sintered from 2090 to 2190 °C in 25 °C steps. After each sintering step the disk was examined using a precision acoustic scanning system to determine acoustic attenuation and velocity. The bulk density was found to vary nonmonotonically with sintering temperature. During the sintering process, the density varied as much as 10 percent from its value at 2090 °C. Local density fluctuations were observed to occur in an organized and history-dependent way. These local density fluctuations varied by up to ±7 percent of the bulk density and were made visible by acoustic attenuation and velocity mapping.

Introduction

Ceramic processing is being extensively investigated by an international effort. The major goal of current processing research is to achieve ceramics, in particular monolithic ceramics, with low porosities (ref. 1). Low porosity ceramics have been produced in recent years. However, it has been found that these dense ceramics still contain large voids sparsely scattered throughout the bulk of the sample. Because of this dilute distribution, these large voids have a negligible effect on the resultant density of the ceramic. Unfortunately, large voids are known to be failure-causing sites in ceramics.

Considerable effort is being made to remove these failure-causing voids by modifying the ceramic powder processing that is done to form green, or unsintered, ceramics. Milling techniques, powder size distributions, binders, pressing pressures, etc., all have an effect on the final density and mean pore size of a sintered ceramic. There are relationships between the type of powder processing and the final microstructure of the sintered ceramic (ref. 2).

We will show that large local density fluctuations occur within the bulk ceramic during sintering. These local density variations are history dependent and can be tracked, or followed, during the sintering process.

Background

Ultrasonic velocity and attenuation are useful as a nondestructive means for determining porosity fraction and for determining the location of large pores or clusters of pores in ceramics. The velocity is linearly related to the density (refs. 3 to 5), and high attenuation is usually attributed to the presence of large pores, clusters of pores, and grain boundary scattering (refs. 6 to 7).

Accurate determination of ultrasonic velocity and attenuation in ceramics requires precise measurements of acoustic waveforms. A precision acoustic scanning system (PASS) (ref. 8) has been constructed for this purpose and is described elsewhere. Briefly, an ultrasonic wave transmitter-receiver (50-MHz broadband transducer) is scanned over the surface of the ceramic. After collection and subsequent Fourier analysis of the appropriate waveforms, an accurate determination of velocity and attenuation can be made (ref. 9). This is done at different positions on the ceramic in an organized array. The resultant data yield velocity and attenuation maps that reveal the porosity variations within the bulk of the ceramic.

Experimental

Sample

A silicon carbide ceramic disk was produced by powder processing, isostatically cold pressed at 60 ksi (414 MPa) and subsequently sintered at 2090 °C for 0.5 hr at 1 atm (6.9 Pa) in argon. The disk was 38 mm diameter by 4 mm with a density of 2.99 g/cm^3. After sintering, the disk was machined to ±0.0011 cm. One side of the disk was polished to a mirror finish with a 3.0-μm-diameter diamond slurry. The polishing was done to provide good acoustic and physical contact between the ultrasonic transducer and the ceramic surface.

Description of Experiment

The disk was sintered, at the same pressure and for the same time, from 2090 to 2190 °C in 25 °C steps. After each step the disk was polished to a mirror finish and acoustically scanned. Approximately 100 μm were removed during polishing. The area scanned was a 20 by 20 mm square, in 250-μm steps, centered at the center of the disk (fig. 1). A 50-MHz, broadband transducer with a 0.31-cm-diameter element and 1.27-cm-long buffer rod was used. A full scan of the entire disk produces permanent damage to the transducer. The damage is done by the transducer scraping over the outer edge of the sample. Therefore, only the central square area was scanned.

After the last scan was done the sample was sectioned horizontally across the diameter. The cross section was obliquely lighted to reveal porosity variations and photographed.

Results

The velocity maps for temperatures 2090, 2115, and 2190 °C are shown in figures 1 to 3, respectively. The acoustic velocity has been previously found to be linearly related to density (refs. 5 to 7), so that reference to high or low velocity may be interchanged with high or low density, respectively. Therefore, these velocity maps also represent density maps. At 2090 °C there is a low velocity (low density) pear-shaped central region surrounded by a high velocity (high density) area. The variation in velocity (density) over this mapped region is ±1 percent from the mean. The velocity map for the next sintering temperature of 2115 °C (fig. 2) exhibits a larger high velocity (high density) pear-shaped region at the center. This central region is surrounded by a low velocity (low density) area. This is in contrast to the previous result that exhibited a low velocity (low density) central region. There exists a sharp boundary outlining the pear-shaped region. This boundary corresponds to a region where there is a large velocity (density) gradient. Within the high velocity (high density) pear-shaped region there is also a low velocity (low density) fluctuation. This sintering temperature yielded the largest variation in

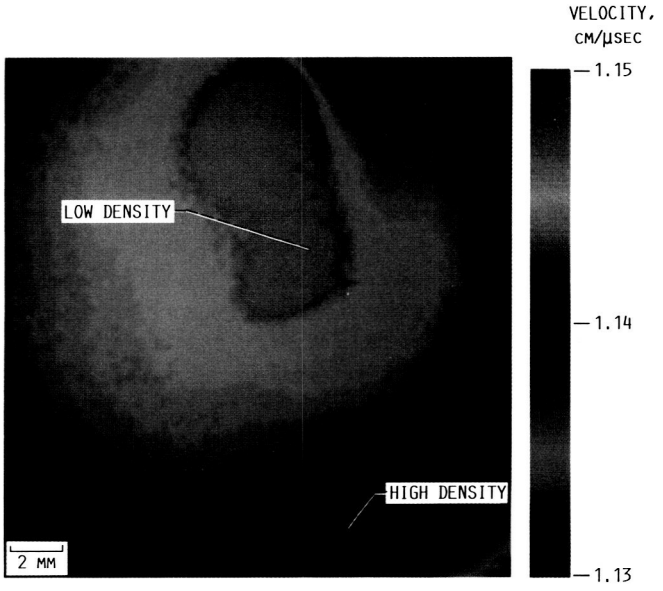

Figure 1.—Velocity map at 50 MHz for 2090 °C sintering step.

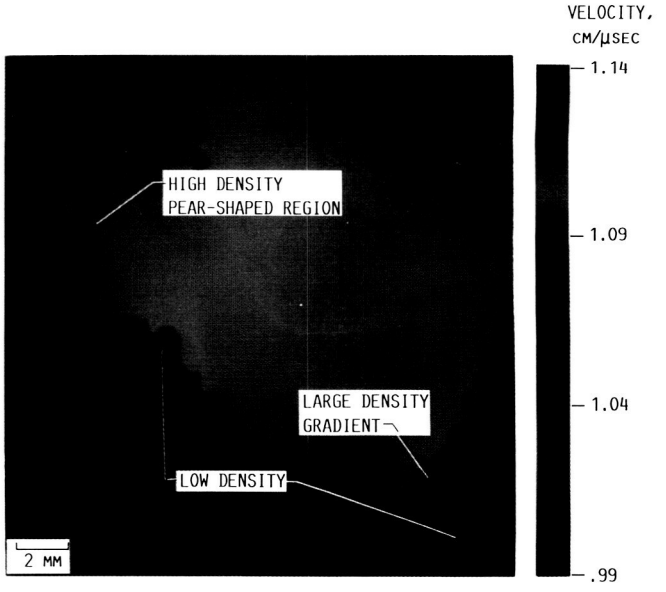

Figure 2.—Velocity map at 50 MHz for 2115 °C sintering step.

velocity (density) of ±7 percent from the mean over the area scanned. The high velocity (high density) pear-shaped region has grown beyond the area scanned at 2190 °C (fig. 3). A low velocity (low density) region has formed within the central region. Note that this new low density region is at a different position than the one indicated at 2115 °C. The variation in velocity (density) over this mapped region is ±3.5 percent from the mean. The horizontal line across the center of the image indicates where the sample was sectioned.

Figure 4 shows the mean velocity over the area scanned and the bulk density of the entire sample as a function of sintering temperature. The vertical bars on the mean velocity curve

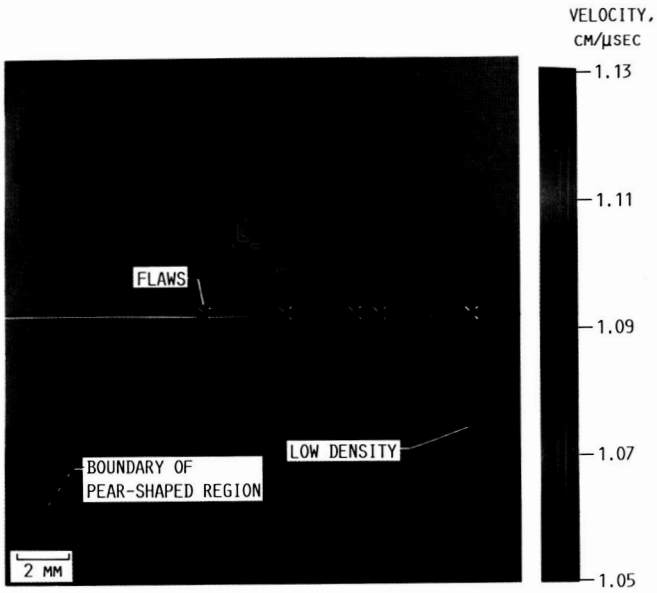

Figure 3.—Velocity map at 50 MHz for 2190 °C sintering step.

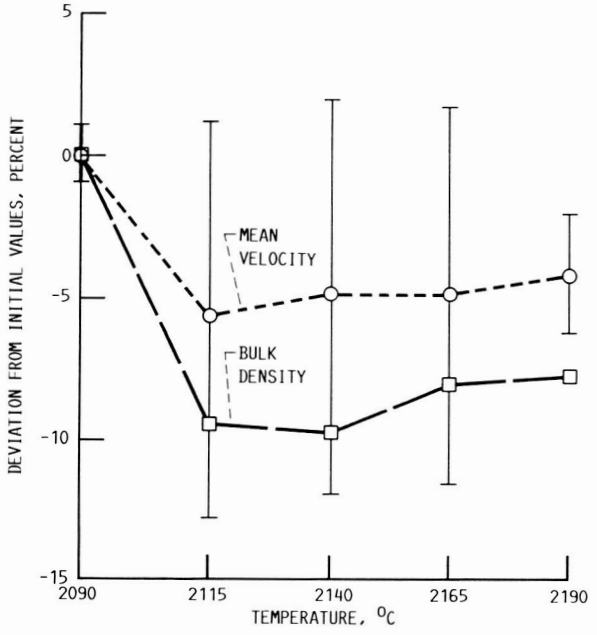

Figure 4.—Deviations of mean velocity and bulk density from their initial values as function of sintering step temperature.

indicate the range of velocities observed (in percent of the mean velocity) over the scanned area.

The attenuation maps for 2090, 2115, and 2190 °C are shown in figures 5 to 7, respectively. At 2090 °C the attenuation map is rather bland. A localized high attenuating region is seen at the center of the upper edge. The attenuation map at 2115 °C shows a high attenuating pear-shaped outline that roughly follows the perimeter of the high velocity pear-shaped region (fig. 2) observed at the same temperature. The highest sintering temperature of 2190° yielded an attenuation map that

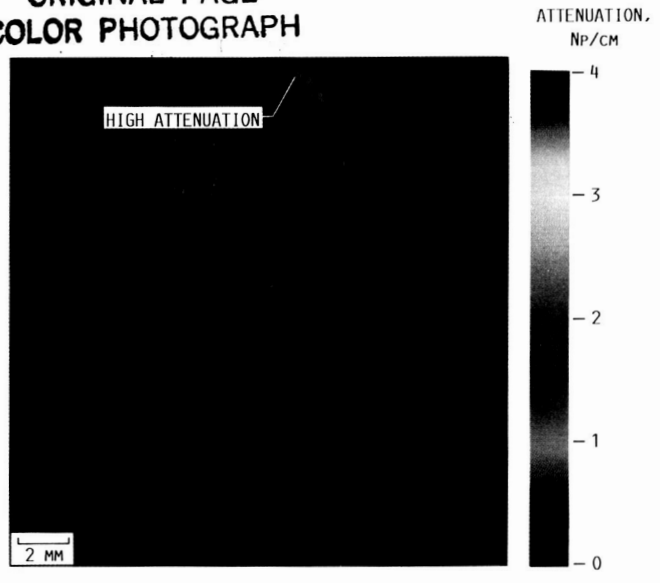

Figure 5.—Attenuation map at 50 MHz for 2090 °C sintering step.

is covered with a collection of organized high attenuation "islands" and strings of "islands."

Figure 8 shows the attenuation, velocity, optical intensity, and photomicrographs for the cross section across the center of the sample. The optical image of the cross section is shown in the center of the figure. The sample has been sectioned in half. The two halves have been placed together so that the scanned surface is at the top and bottom of the photo. The optical intensity curve was obtained by integrating the optical intensity vertically along the cross section. The optical data has been inverted so that the depression in the optical curve corresponds to a decrease in the density. The velocity along the same path shows a depression at the same position as the

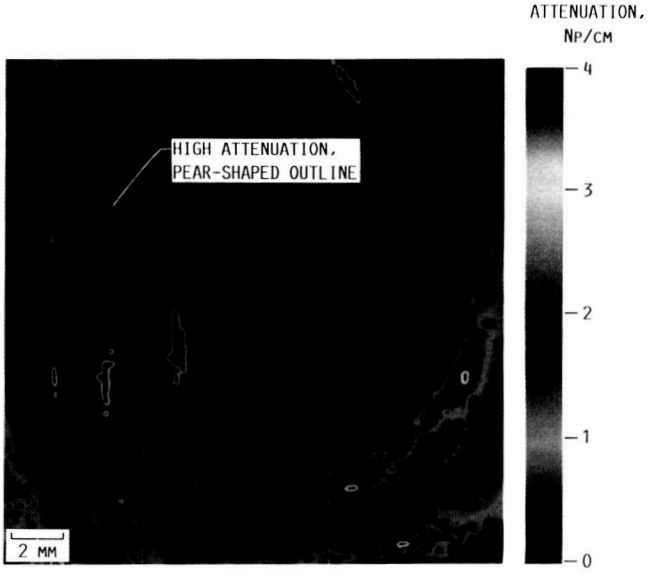

Figure 6.—Attenuation map at 50 MHz for 2115 °C sintering step.

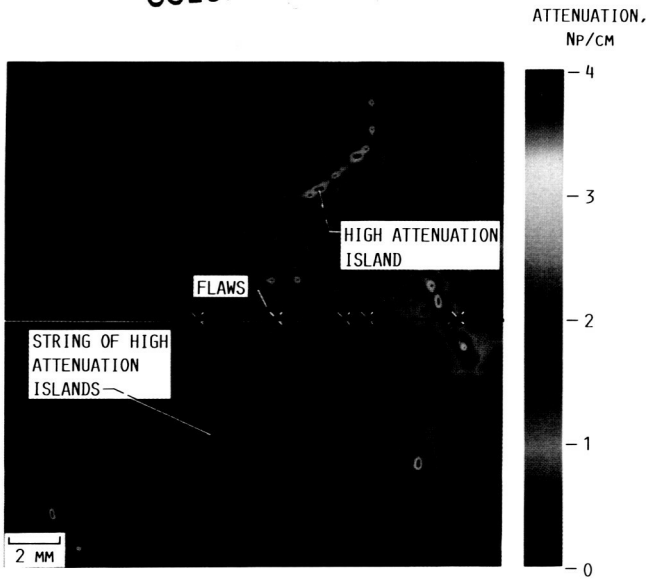

Figure 7.—Attenuation map at 50 MHz for 2190 °C sintering step.

low density region observed optically. The attenuation exhibits peaks at regions where there are gradients in both velocity and density.

In the cross section, the pore sizes ranged from 3 to 15 μm. Five anomalously large (40 to 75 μm) pores were found within this cross-sectional area. The locations of these large voids are indicated by the arrows in figure 8 and by the X's in figures 3 and 7.

Discussion

Both the mean velocity and the density decreased from the initial starting sinter. After reaching minimum values both the mean velocity and density began to increase. The mean velocity does not follow the bulk density exactly. This is as expected, since the mean velocity is only determined from the area scanned and not from the entire sample. Using the mean velocity and bulk density results, we observe the density of the sample varies nonmonotonically with temperature during the sintering process.

In addition to the mean velocity and bulk density variations with sintering temperature, we observed local fluctuations in velocity in the area scanned (figs. 2 to 4 and 8). These variations, ranging from ± 1 to ± 7 percent from the mean, correspond to similar variations in the local density. The largest variation in velocity occurred near the minimum of the mean velocity and at the 2115 °C sintering temperature.

As the sintering temperature was increased, the relatively smooth-edged, pear-shaped region in the velocity map at 2090 °C (fig. 2) formed sharp edges and eventually grew to be larger than the area that was being scanned. This is an indication that these variations are history dependent and are not occurring spontaneously.

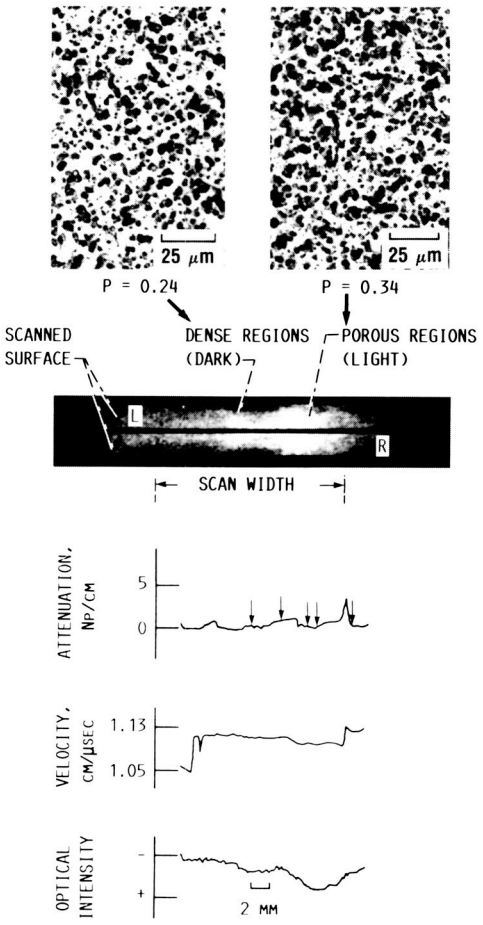

Figure 8.—Optical and ultrasonic interrelationship. Top photomicrographs indicate the porosity fraction, P, along the cross section. Density variations along the cross section are indicated by light (porous) and dark regions (dense) in the center photograph. Graph at bottom shows ultrasonic attenuation and velocity and optical intensity along the cross section. Optical intensity curve has been inverted for direct comparison with velocity.

Regions that show high attenuation generally overlapped the sharp boundaries in the velocity maps. It has been reported previously that grain boundary scattering is negligible for silicon carbide at the ultrasonic frequencies used here (ref. 8). The presence of anomalously large voids is known to yield high attenuation. When comparing figures 7 and 8 it is seen that high attenuation did not necessarily occur at the location of these large voids or at regions of low density (fig. 8). In particular there is a minimum in the attenuation at the region of lowest density. This minimum is between the two largest peaks in the attenuation shown in figure 8 and also is the lightest area in the photograph of the cross section. High attenuation is observed where there are large spatial variations or gradients in the velocity or density (figs. 3, 7, and 8).

Refraction of waves occurs at boundaries that are impedance mismatched. For planar boundaries, a refracted wave leaves the boundary at an angle determined by the well-known Snell's law. It should be remembered that the acoustic

impedance, $Z(r) = \rho(r)V(r)$, at an arbitrary point r within the sample includes both the local density $\rho(r)$ and the local acoustic velocity $V(r)$. Since there are large density and velocity gradients (figs. 3, 4, and 8), it is believed that these attenuation maps are maps of "apparent" attenuation caused by refractive scattering at these high gradient regions (ref. 10). The acoustic energy is being redirected, because of refraction from the main acoustic beam, and results in an "apparent" attenuation.

The refractive scattering effects may lead to both high and low values for "apparent" attenuation depending on where the ultrasonic beam is being redirected to. For example, it seems plausible that density variations may exist that tend to focus the ultrasonic beam. This focusing may result in an enhancement of the ultrasonic wave and yield a low value in the "apparent" attenuation. Therefore, regions of high "apparent" attenuation may indicate the presence of large density gradients and not necessarily isolated large pores or regions of high porosity.

Conclusions

A silicon carbide disk was sintered from 2090 to 2190 °C in 25 °C steps. After each sintering step the disk was examined using a precision acoustic scanning system to determine acoustic attenuation and velocity. The bulk density was found to vary nonmonotonically with sintering temperature. During the sintering process, the density varied as much as 10 percent from its value at 2090 °C. Local density fluctuations were observed to occur in an organized and history-dependent way. These local density fluctuations varied by up to ± 7 percent of the bulk density and were made visible by acoustic attenuation and velocity mapping.

References

1. Richardson, D.W.: Modern Ceramic Engineering. Marcel Dekker, 1982.
2. Structural Ceramics, NASA CP-2427, 1986.
3. Papadakis, E.P.; and Peterson, B.W.: Ultrasonic Velocity as a Predictor of Density in Sintered Powder Metal Parts. Mater. Eval., vol. 37, no. 5, Apr. 1979, pp. 76–80.
4. Klima, S.K.; et al.: Ultrasonic Velocity for Estimating Density of Structural Ceramics. NASA TM-82765, DOE/NASA/51040-35, 1981.
5. Wang, S.; and Adler, L.: Ultrasonic Studies of Strength-Related Properties of Graphite. Review of Progress in Quantitative Nondestructive Evaluation, Vol. 3B, D.O. Thompson and D.E. Chimemti, eds., Plenum Press, 1984, pp. 1211–1219.
6. Rose, J.H.: Kramers-Kronig Relations and the Ultrasonic Characterization of Porosity. Review of Progress in Quantitative Nondestructive Evaluation, Vol. 5B, D.O. Thompson and D.E. Chimemti, eds., Plenum Press, 1986, pp. 1617–1623.
7. Papadakis, E.P.: Ultrasonic Attenuation Caused by Scattering in Polycrystalline Metals. J. Acoust. Soc. Am., vol. 37, no. 4, Apr. 1965, pp. 711–717.
8. Generazio, E.R.; Roth, D.J.; and Baaklini, G.Y.: Acoustic Imaging of Subtle Porosity Variations in Ceramics, Mater. Eval, vol. 46, no. 10, Sept. 1988, pp. 1338–1343.
9. Generazio, E.R.: The Role of the Reflection Coefficient in Precision Measurement of Ultrasonic Attenuation, Mater. Eval., vol. 43, no. 8, July 1985, pp. 995–1004.
10. Telschow, K.; Walter, J.; and Kunerth, D.: Ultrasonic Characterization of Nonuniform Porosity Distribution in SiC Ceramic. Review of Progress in Quantitative Nondestructive Evaluation, Vol. 7B, D.O. Thompson and D.E. Chimemti, eds., Plenum Press, 1988, pp. 1285–1292.

NASA
National Aeronautics and Space Administration

Report Documentation Page

1. Report No.	2. Government Accession No.	3. Recipient's Catalog No.
NASA TM-101340		

4. Title and Subtitle	5. Report Date
Dynamic Porosity Variations in Ceramics	December 1988
	6. Performing Organization Code

7. Author(s)	8. Performing Organization Report No.
Edward R. Generazio, David B. Stang, and Don J. Roth	E-4358
	10. Work Unit No. 506-43-11

9. Performing Organization Name and Address	11. Contract or Grant No.
National Aeronautics and Space Administration Lewis Research Center Cleveland, Ohio 44135-3191	
	13. Type of Report and Period Covered Technical Memoradum
12. Sponsoring Agency Name and Address	
National Aeronautics and Space Administration Washington, D.C. 20546-0001	14. Sponsoring Agency Code

15. Supplementary Notes

Edward R. Generazio and Don J. Roth, NASA Lewis Research Center; David B. Stang, Sverdrup Technology, Inc., NASA Lewis Research Center Group, Cleveland, Ohio 44135.

16. Abstract

A silicon carbide disk was sintered from 2090 to 2190 °C in 25 °C steps. After each sintering step the disk was examined using a precision acoustic scanning system to determine acoustic attenuation and velocity. The bulk density was found to vary nonmonotonically with sintering temperature. During the sintering process, the density varied as much as 10 percent from its value at 2090 °C. Local density fluctuations were observed to occur in an organized and history-dependent way. These local density fluctuations varied by up to ±7 percent of the bulk density and were made visible by acoustic attenuation and velocity mapping.

17. Key Words (Suggested by Author(s))	18. Distribution Statement
Density; Porosity; Ceramics; Ultrasonic; Attenuation; Velocity; Sintering; Silicon carbide; Structural ceramics; Silicon nitride	Unclassified – Unlimited Subject Category 27

19. Security Classif. (of this report)	20. Security Classif. (of this page)	21. No of pages	22. Price*
Unclassified	Unclassified	8	A02

NASA FORM 1626 OCT 86

*For sale by the National Technical Information Service, Springfield, Virginia 22161